CRYSTAL GROWTH & DESIGN
2006
VOL. 6, NO. 8
1967−1971

Mesh-Like Hemispherical Shells Formed by Self-Assembly of Zn_2SiO_4 Textured Nanowires

Xiaohong An, Guowen Meng,* Qing Wei, and Lide Zhang

Key Laboratory of Materials Physics and Anhui Key Laboratory of Nanomaterials and Nanostructures, Institute of Solid State Physics, Chinese Academy of Sciences, Hefei 230031, P. R. China

Received February 28, 2006; Revised Manuscript Received May 12, 2006

ABSTRACT: A new kind of self-assembled nanostructures, mesh-like hemispherical shells consisting of Zn_2SiO_4 nanowires, was synthesized by a simple thermal evaporation and condensation process. X-ray diffraction and scanning electron microscopy characterizations on the products obtained at different stages during the thermal evaporation indicate that the mesh-like hemispherical shells were formed through generation of Zn vapor, solidification of liquid Zn droplets, surface oxidization, sublimation, splitting into hemispherical porous shells, further sublimation and oxidization, and reaction with SiO_x vapor to form Zn_2SiO_4. The corresponding photoluminescence (PL) measurements reveal that the evolution of the mesh-like hemispherical shells accompanied the conversion of emissions at 385 and 508 nm from ZnO phase into emission at 522 nm from Zn_2SiO_4 phase. The novel Zn_2SiO_4 self-assembled nanostructures might have potential applications in future gas sensor and optoelectronic nanodevices.

Introduction

Assembling nanoscale building blocks into desired architectures is a significant challenge in advanced nanodevices[1,2] and has potential in optical, microelectronic, sensing, chemical, and biological applications.[3] By use of solution-based chemical approaches, various architectures consisting of size- and shape-controlled nanocrystals have been self-assembled for a wide range of metals,[4−9] semiconductors,[10−12] and oxides.[13] However, exploring a simple approach to self-assembled nanostructures is still interesting to chemists and material scientists.

Zinc silicate (Zn_2SiO_4), with a wide band gap of 5.5 eV, is a promising multifunctional material. It has a wide range of applications such as phosphor host,[14] paints,[14] important crystalline phase in glass ceramics,[15] electronic insulators,[16] and rubber mixtures.[17,18] Especially, Zn_2SiO_4-based nanostructures have been widely studied in recent years due to their importance to the study of size- and dimensionality-dependent chemical and physical properties and great potential applications.[19,20] For example, mesoporous single-crystal ZnO sheathed with Zn_2SiO_4 nanowires,[21] highly aligned Mn-doped Zn_2SiO_4 nanorods,[22] and aligned $Zn-Zn_2SiO_4$ core−shell nanocables[23] have been obtained by a chemical vapor deposition technique. Additionally, Mn-doped Zn_2SiO_4 rodlike nanoparticles have been synthesized through a hydrothermal method.[24]

Here we demonstrate the synthesis of mesh-like hemispherical shells formed by self-assembly of textured Zn_2SiO_4 nanowires via a simple thermal evaporation and condensation process. As a new promising route for fabricating self-assembled nanostructures, this method might be exploited to obtain other fancy architectures of desired materials and enhance realization of nanodevices. Photoluminescence (PL) spectra taken from the mesh-like Zn_2SiO_4 hemispherical shells reveal a strong peak at 522 nm, indicating that the novel Zn_2SiO_4 nanostructures might have potential applications in future gas sensor and optoelectronic nanodevices.

Experimental Section

The mesh-like hemispherical shells consisting of Zn_2SiO_4 nanowires were obtained by using a simple thermal evaporation method. Mixed powders of $ZnCO_3$ (99.9 wt %, 1.05 g) and black carbon (97 wt %, 0.18 g) loaded in a ceramic boat were put into the hot zone of a horizontal tube furnace. A Si wafer (5×5 mm^2) was ultrasonically cleaned in ethanol and then placed at the downstream side of the source materials at a distance of about 11 cm. The furnace was heated from room temperature to 1100 °C in 12 min and maintained at this temperature for different periods of time (5−60 min). High-purity Ar (99.99%, $O_2 \approx 0.01\%$) at a flow rate of 5 mL/min was introduced into the furnace during the thermal evaporation process. The temperature of the Si substrate is about 600 °C determined by a premeasured temperature gradient curve. After the furnace was cooled to room temperature, white products were found on the Si wafer, and characterized by scanning electron microscopy (SEM, Sirion 200) and high-resolution transmission electron microscopy (HRTEM, JEOL 2010 at 200 kv). Energy-dispersive X-ray spectroscopy (EDS) attached to the HRTEM and X-ray diffraction (XRD, X'Pert Pro MPD) were employed to confirm the components of the products. Photoluminescence spectra of the products on the Si wafer were recorded on a LabRam-HR microRaman spectrometer (Jobin-Yvon).

Results and Discussion

Low-magnification SEM observation (Figure 1a) of the white products on the Si wafer after thermal evaporation for 60 min reveals that the Si wafer is covered with flabby hemispherical shells with diameters ranging from several tens to hundreds of micrometers. High-magnification SEM observation (Figure 1b) of a single hemispherical shell with diameter about 30 μm shows that the shell of the hemisphere is not compact but porous, and collapses and distortions can be seen on the hemispherical shells. A close-up view (Figure 1c) of the porous shell displays mesh-like structures textured by interconnected curved nanowires.

A low-magnification TEM image (Figure 2a) of broken fragments of the mesh-like hemispherical shell after sonication further shows that the mesh-like hemispherical shell is formed by self-assembly of textured nanowires that are several tens of nanometers in width and several hundreds of nanometers in length. Selected area electron diffraction (SAED) patterns taken from different areas of the fragments show similar patterns, revealing that the components and structure of the textured nanowires are uniform. The SAED pattern taken along the [$\bar{1}$ 1 0 1] zone axis (Figure 2b) can be indexed to rhombohedral structured Zn_2SiO_4 with (1 1 0) and (1 0 1). The corresponding HRTEM image (Figure 2c) shows a lattice fringe spacing about 0.742 nm perpendicular to the growth direction, further revealing

* To whom correspondence should be addressed. E-mail: gwmeng@issp.ac.cn.

10.1021/cg060106r CCC: $33.50
Published on Web 06/24/2006

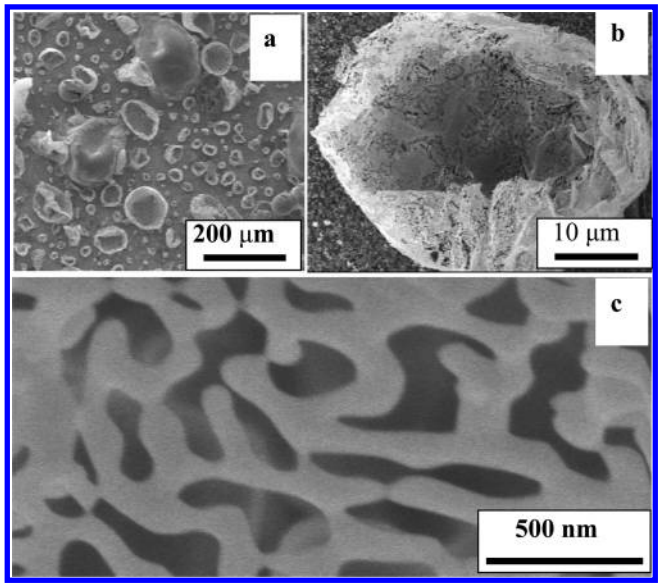

Figure 1. SEM images of the as-synthesized mesh-like hemispherical shells: (a) low magnification; (b) medium magnification; (c) high magnification.

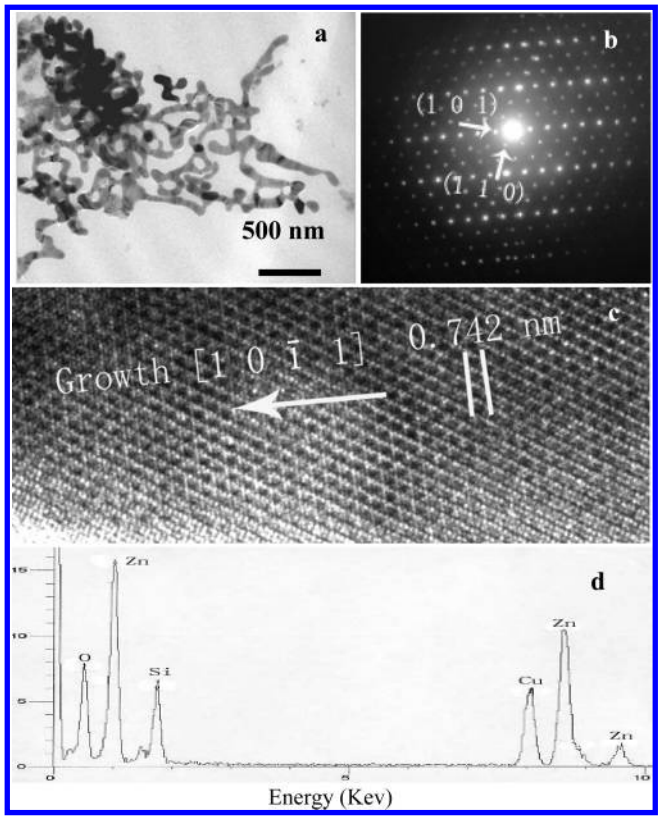

Figure 2. TEM image (a) of the broken fragments of the mesh-like hemispherical shells, SAED pattern (b) of the Zn_2SiO_4 nanocrystals, HRTEM image (c) of the Zn_2SiO_4 nanocrystals, and EDS (d) of the Zn_2SiO_4 nanocrystals.

that the nanowires are composed of Zn_2SiO_4 and grow along the [1 0 $\bar{1}$ 1] direction. Energy-dispersive X-ray spectrometry (EDS) analysis indicates that each nanowire is composed of Zn, O, and Si. The peaks of Cu come from the Cu grids.

X-ray diffraction (XRD) analyses were carried on the products achieved after thermal evaporation of the mixed powders for different periods of time to get information about the evolution of the phase transformation from mixed powders to mesh-like hemispherical shells consisting of Zn_2SiO_4 nanowires. Figure

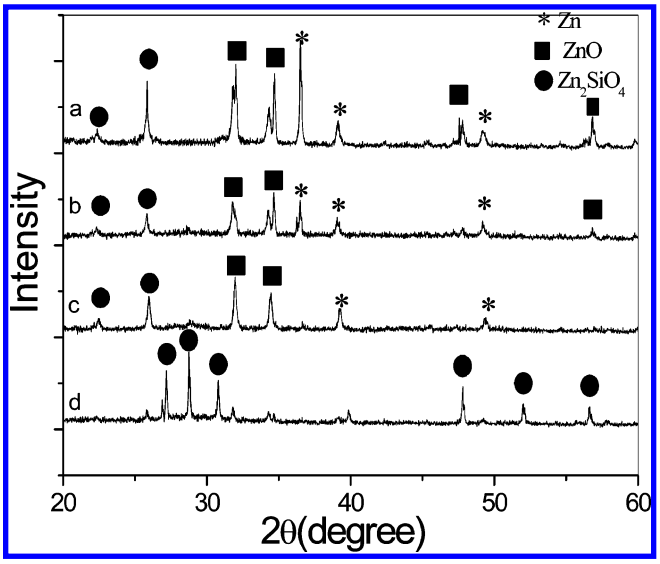

Figure 3. XRD patterns of the products obtained after thermal evaporation for different periods of time: (a) 5, (b) 20, (c) 40, and (d) 60 min.

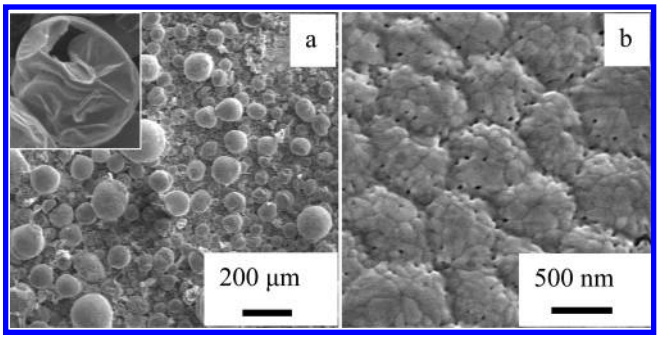

Figure 4. SEM images of the product after the thermal evaporation was performed for 5 min.

3 shows a series of XRD patterns of the products obtained after evaporation for 5, 20, 40, and 60 min, respectively. After evaporation for 5 min, the obtained XRD pattern (curve a in Figure 3) reveals that the main peaks can be indexed to the hexagonal structure of Zn and ZnO, with minor peaks being indexed to the rhombohedral structure of Zn_2SiO_4. With the increase of evaporation time, the intensity of the Zn phase decreases rapidly, while the relative intensity of the ZnO and Zn_2SiO_4 increases. After reaction for 60 min, all the peaks in the XRD pattern (curve d in Figure 3) can be indexed to the Zn_2SiO_4 phase. Therefore it can be concluded that metallic Zn was first oxidized into ZnO and then entirely transformed into Zn_2SiO_4 after thermal evaporation for 60 min.

To further study the growth process of mesh-like hemispherical shells consisting of Zn_2SiO_4 nanowires, SEM observations were carried out on the products obtained for different periods of reaction time. After evaporation for 5 min, a low-magnification SEM image (Figure 4a) reveals that numerous microspheres with diameters ranging from several tens of micrometers to several hundreds of micrometers, were self-assembled on the Si wafer. The inset shows the SEM image of a broken sphere, revealing that the microsphere is hollow. High-magnification SEM image (Figure 4b) of one hollow microsphere indicates that the shell is made up of numerous nanocrystals. Taking XRD analysis (curve a in Figure 3) and SEM observation together, these nanocrystals are mainly composed of ZnO and Zn.

After thermal evaporation for 20 min, a large quantity of slightly collapsed and distorted hollow hemispherical shells is

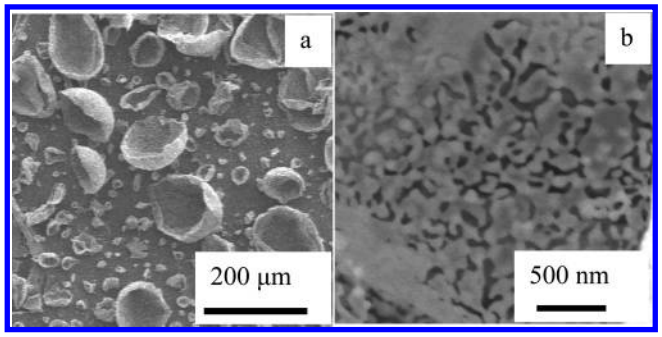

Figure 5. SEM images of the product after the thermal evaporation was performed for 20 min.

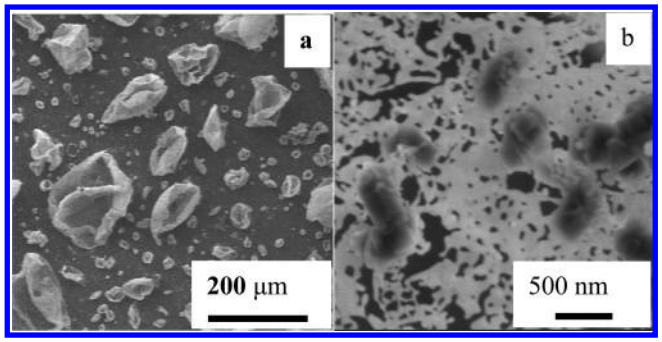

Figure 6. SEM images of the product after the thermal evaporation was performed for 40 min.

obtained (Figure 5a). It can be seen that the hemispherical shells range from several tens of micrometers to hundreds of micrometers in diameter. The XRD analysis (curve b in Figure 3) reveals that the hollow hemispherical shells are still mainly composed of Zn/ZnO. Figure 5b is the high-magnification image of the surface of one hemispherical shell, indicating that the hemispherical shells are mainly textured by nanocrystals with a few short nanowires among them. Since Zn has a much lower melting point of 419 °C, further thermal evaporation led to the sublimation and oxidation of Zn nanocrystals constituting the Zn/ZnO hollow microsphere shells, resulting in thin and flabby porous spherical shells consisting of nanocrystals and nanowires. Because of gravitation, the porous hollow sphere shells of Zn/ZnO collapsed or split into hemispherical porous shells from the thinner and flabbier area on the porous sphere shells.

Further thermal evaporation led to further sublimation and oxidation of Zn nanocrystals in the hemispherical shells. So the obtained hemispherical shells became thinner and flabbier, resulting in serious transformation of the hemispherical shells. From Figure 6a, it can be observed that the hemispherical shells become too flabby to remain the shape of a hemisphere under gravity. The corresponding XRD analysis (curve c in Figure 3) indicates that the Zn phase is drastically reduced and the ZnO phase becomes the main components of the hemispherical shells. The close-up view (Figure 6b) of one distorted hemispherical shell further displays that most of nanocrystals in the hemispherical shell are transformed into nanowires. With the prolongation of thermal evaporation, the Zn phase in the hemispherical shells is entirely oxidized and reacted with SiO_x vapor, resulting in the mesh-like Zn_2SiO_4 hemispherical shells.

On the basis of the above analysis, we proposed a reasonable formation process for the mesh-like hemispherical shells textured by Zn_2SiO_4 nanowires as shown schematically in Figure 7, which is similar to the formation of the ZnO cages and shells reported by the Wang group.[25] During the evaporation, $ZnCO_3$ powders are initially heated to generate ZnO and CO_2 vapor.

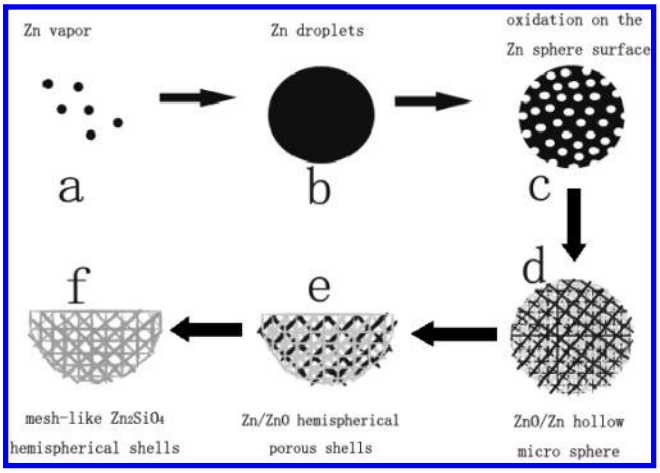

Figure 7. Schematic illustration of the formation of the mesh-like hemispherical shells formed by textured self-assembly of Zn_2SiO_4 nanowires (the black color stands for Zn; the white color stands for ZnO; the gray color stands for Zn_2SiO_4).

Then ZnO reacts with C (graphite) to form Zn and CO_2. The Zn vapor was carried to the low-temperature region by Ar gas (shown in Figure 7a). Because the reaction temperature is high, the Zn vapor increases quickly, condenses together, forms liquid clusters, and further grows into liquid droplets on the Si wafer in the low-temperature region. Then the liquid droplets quickly solidify to form Zn spheres. This stage can be reflected in Figure 7b. The surface of the Zn spheres can be easily oxidized and formed randomly interlaced ZnO/Zn sphere surface (displayed in Figure 7c), due to the remaining O_2 in the carrier Ar gas and from the sealing leakage of the ceramic tube furnace. At about 600 °C around the local substrate, the inner core of the Zn spheres is sublimed, forming hollow microscale sphere shells (shown in Figure 7d). Further thermal evaporation leads to the sublimation and oxidization of the Zn nanocrystals constituting the hollow microsphere shells, resulting in thin and flabby microporous sphere shells. Because of the gravitation, the porous microsphere shells collapsed or split into hemispherical porous shells from the thinner and flabbier area on the porous microsphere shells. This step has been clearly depicted in Figure 7e. With the prolongation of reaction, Zn nanocrystals in the hemispherical porous shells are entirely sublimed and oxidized, resulting in the mesh-like hemispherical shells consisting of ZnO nanowires. Meanwhile, the Si vapors sublimated from the Si wafer are oxidized into SiO_x vapors during the reaction. As it has been reported, the electronegativity of Si is 1.9 and that of Zn is 1.65, which are quite close. Additionally, the atomic sizes of Si (0.117 nm) and Zn (0.133 nm) are also comparable. So when the SiO_x vapor deposits on the ZnO nanowires surface, they can quickly diffuse into the ZnO lattice and form a new phase Zn_2SiO_4, being similar to the formation of mesoporous single-crystal ZnO nanowires sheathed with Zn_2SiO_4.[21] With the prolongation of thermal evaporation, ZnO nanowires completely react with SiO_x vapors and transform into Zn_2SiO_4 nanowires constituting the mesh-like hemispherical shells, as indicated in Figure 7f. It can be concluded that the formation of mesh-like hemispherical shells consists of generation of Zn vapors, solidification of liquid droplets, surface oxidization, sublimation, splitting into hemispherical porous shells, further sublimation and oxidization, reaction with SiO_x vapor, and formation of Zn_2SiO_4.

Photoluminescence (PL) spectra from the products obtained for different periods of reaction time are measured at room temperature with the excitation wavelength of 325 nm. It was

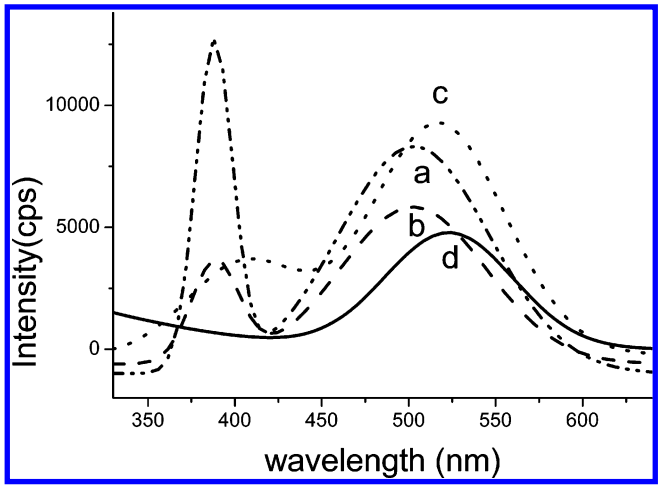

Figure 8. The PL spectra of the products obtained after thermal evaporation for different periods of time: 5 min (—••, curve a), 20 min (— — —, curve b), 40 min (•••, curve c), and 60 min (—, curve d).

found that the evolution of the mesh-like hemispherical shells during the thermal evaporation accompanied changes in the emission characteristics in the PL spectra. Curves a—d in Figure 8 are the PL spectra of the products obtained after thermal evaporation for 5 min (dash—dot—dot, curve a), 20 min (dash, curve b), 40 min (dot, curve c), and 60 min (solid, curve d). It can be seen that the obtained products for different periods of reaction time have three different emissions, an ultraviolet one centered at 385 nm and two different green emissions at 508 and 522 nm. The UV emission band (385 nm) corresponds to the near band edge peak that is attributed to the recombination of free excitons of ZnO.[26] The green emission band at 508 nm originates from the recombination of the holes with the electrons occupying the singly ionized oxygen vacancy in ZnO.[27−29] Additionally, the green peak located at 522 nm is attributed to Zn_2SiO_4.[30] Curve a and b in Figure 8 show two similar emissions of 385 and 508 nm, which are consistent with previous results on other ZnO nanostructures.[31] Based on the corresponding XRD analysis (curves a and b in Figure 3), it can be predicted that the ZnO phase in Zn/ZnO spherical shells produces these two emissions. With the prolongation of the thermal evaporation, the intensity of 385 nm emission decreases and the relative intensity of the 508 nm emission increases, which may be ascribed to the oxygen deficiencies on the increased surface area and interfaces among the spherical shells consisting of the ZnO nanowires transformed from Zn nanocrystals. Curves c and d in Figure 8 reveal one similar emission of 522 nm, except for the UV emission of 385 nm in curve c. With the further prolongation of the thermal evaporation, the emission peak at 385 nm gradually disappears, while the relative intensity of the 522 nm emission is drastically increased. This change in PL spectra may be attributed to the transformation from ZnO nanowires into Zn_2SiO_4 nanowires after further thermal evaporation, being consistent with the results from the XRD analyses (curves c and d in Figure 3). Based on the above PL spectra, it can be concluded that the oxygen deficiencies from ZnO on the increased surface area and interfaces among the spherical shells during the first 20 min thermal evaporation results in the decrease of the intensity of 385 nm emission and the increase of the relative intensity of 508 nm emission, while the transformation of the ZnO phase into the Zn_2SiO_4 phase in the further thermal evaporation, creating the increase of defects for 522 nm emission, leads to the conversion of emissions at 385 and 508 nm into emission at 522 nm. The final products of Zn_2SiO_4 hemispherical shells display mesh-like structure and a strong emission of 522 nm, revealing that the novel self-assembled nanostructures might have potential applications in future gas sensor and optoelectronic nanodevices.

Conclusion

In summary, mesh-like hemispherical shells formed by self-assembly of textured Zn_2SiO_4 nanowires have been obtained during thermal evaporation. The formation of this novel self-assembly nanostructure consists of generation of Zn vapors, solidification of liquid droplets, surface oxidization, sublimation, splitting into hemispherical porous shells, further sublimation and oxidization, and reaction with SiO_x vapor to form mesh-like Zn_2SiO_4 hemispherical shells. PL spectra recorded on the mesh-like Zn_2SiO_4 hemispherical shells show a strong peak at 522 nm, indicating that the novel self-assembly nanostructures have potential optoelectronic applications in the future nanotechnology.

Acknowledgment. This work was supported by the Natural Science Foundation of China (Grant Nos. 10374092 and 50525207) and the Ministry of Sciences and Technology of China (Grant No. 2005CB623603)

References

(1) Huang, Y. X.; Duan, F.; Wei, Q. Q.; Lieber, C. M. *Science* **2001**, *291*, 630.
(2) Hamley, I. W. *Angew. Chem., Int. Ed.* **2003**, *42*, 1692.
(3) Shipway, A. N.; Katz, E.; Willner, I. *ChemPhysChem* **2000**, *1*, 18.
(4) Whetten, R. L.; Khoury, J. T.; Alvarez, M. M.; Murthy, S.; Vezmar, I.; Wang, Z. L.; Stephens, P. W.; Cleveland, C. L.; Luedtke, W. D.; Landman, U. *Adv. Mater.* **1996**, *8*, 428.
(5) Collier, C. P.; Saykally, R. J.; Shiang, J. J.; Henrichs, S. E.; Heath, J. R. *Science* **1997**, *277*, 1978.
(6) Pileni, M. P. *Appl. Surf. Sci.* **2001**, *171*, 1.
(7) Pileni, M. P. *J. Phys. Chem. B* **2001**, *105*, 3358.
(8) Sun, S. H.; Murray, C. B.; Weller, D.; Folks, L.; Moser, A. *Science* **2000**, *287*, 1989.
(9) Kiely, C. J.; Fink, J.; Brust, M.; Bethell, D.; Schiffrin, D. J. *Nature* **1998**, *396*, 444.
(10) Murray, C. B.; Kagan, C. R.; Bawendi, M. G. *Science* **1995**, *270*, 1335.
(11) Peng, X. G.; Manna, L.; Yang, W. D.; Wickham, J.; Scher, E.; Kadavanich, A.; Alivisatos, A. P. *Nature* **2000**, *404*, 59.
(12) Braun, P. V.; Osenar, P.; Stupp, S. I. *Nature* **1996**, *380*, 325.
(13) Yin, J. S.; Wang, Z. L. *Phys. Rev. Lett.* **1997**, *79*, 2570.
(14) Bartohu, C.; Benoit, J.; Benalloul, P.; Morell, A. *J. Electrochem. Soc.* **1994**, *141*, 524.
(15) Strand, Z. *Glass Sci. Technol.* **1986**, *8*, 101.
(16) Lepkova, D.; Nenor, A.; Pavlova, I. *Stroit. Mater. Silik. Promst.* **1980**, *21*, 18.
(17) Krysztafkiewicz, A.; Michalska, I.; Jesionowski, T. *Compos. Interfaces* **2001**, *8*, 257.
(18) Michalska, I.; Krysztafkiewicz, A.; Bogacki, M. B.; Jesionowski, T. *J. Chem. Technol. Biotechnol.* **2003**, *78*, 452.
(19) Han, J.; Fan, S.; Li, Q.; Hu, Y. *Science* **1997**, *277*, 1287.
(20) Ruecks, T.; Kim, K.; Joselevich, E.; Tseng, G. Y.; Cheung, C.; Lieber, C. M. *Science* **2000**, *289*, 94.
(21) Wang, X. D.; Summers, C. J.; Wang, Z. L. *Adv. Mater.* **2004**, *16*, 1215.
(22) Yang, L. W.; Wu, X. L.; Huang, G. S.; Qiu, T.; Yang, Y. M.; Siu, G. G. *Appl. Phys. A* **2005**, *81*, 929.
(23) Feng, X.; Yuan, X. L.; Sekiguchi, T.; Lin, W. Z.; Kang, J. Y. *J. Phys. Chem. B* **2005**, *109*, 15786.
(24) Wang, H. F.; Ma, Y. Q.; Yi, G. S.; Chen, D. P. *Mater. Chem. Phys.* **2003**, *82*, 414.
(25) Gao, P. X.; Wang, Z. L. *J. Am. Chem. Soc.* **2003**, *125*, 11299.
(26) Kong, Y. C.; Yu, D. P.; Zhang, B.; Fang, W.; Feng, S. Q. *Appl. Phys. Lett.* **2001**, *78*, 407.
(27) (a) Pan, Z. W.; Dai, Z. R.; Wang, Z. L. *Science* **2001**, *291*, 1947. (b) Huang, M.; Wu, Y.; Feick, H.; Tran, N.; Weber, E.; Yang, P. *Adv.*

Mater. **2001**, *13*, 113. (c) Hu, J. Q.; Bando, Y. *Appl. Phys. Lett.* **2003**, *82*, 1401.
(28) Vanheusden, K.; Warren, W. L.; Seager, C. H.; Tallant, D. R.; Voigt, J. A.; Gnade, B. E. *J. Appl. Phys*. **1996**, *79*, 7983.
(29) Wu, X. L.; Siu, G. G.; Fu, C. L.; Ong, H. C. *Appl. Phys. Lett.* **2001**, *78*, 2285.
(30) Xu, X. L.; Wang, P.; Qi, Z. M.; Ming, H.; Xu, J.; Liu, H. T.; Shi, C. S.; Lu, G.; Ge, W. K. *J. Phys.: Condens. Matter* **2003**, *15*, L607.
(31) Shen, G. Z.; Bando, Y.; Lee, C. J. *J. Phys. Chem. B* **2005**, *109*, 10578.

CG060106R